






Diverse structures, magnetism and photoluminescence of four transition metal coordination compounds based on the semirigid 4-(pyridin-3-yloxy)-phthalic acid

Lingling Zhang, Peng Gao, Yanhong Zhang & Ming Hu

To cite this article: Lingling Zhang, Peng Gao, Yanhong Zhang & Ming Hu (2015) Diverse structures, magnetism and photoluminescence of four transition metal coordination compounds based on the semirigid 4-(pyridin-3-yloxy)-phthalic acid, Journal of Coordination Chemistry, 68:21, 3932-3944, DOI: [10.1080/00958972.2015.1081183](https://doi.org/10.1080/00958972.2015.1081183)

To link to this article: <http://dx.doi.org/10.1080/00958972.2015.1081183>

 View supplementary material 

 Accepted author version posted online: 13 Aug 2015.
Published online: 01 Sep 2015.

 Submit your article to this journal 

 Article views: 48

 View related articles 

 View Crossmark data 

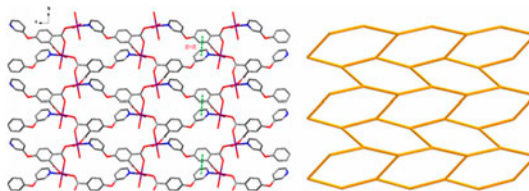
Diverse structures, magnetism and photoluminescence of four transition metal coordination compounds based on the semirigid 4-(pyridin-3-yloxy)-phthalic acid

LINGLING ZHANG[†], PENG GAO[†], YANHONG ZHANG[‡] and MING HU^{*†}

[†]Inner Mongolia Key Laboratory of Chemistry and Physics of Rare Earth Materials, School of Chemistry and Chemical Engineering, Inner Mongolia University, Hohhot, China

[‡]College of Chemistry and Environmental Science, Inner Mongolia Normal University, Hohhot, China

(Received 28 October 2014; accepted 24 July 2015)



Four transition metal coordination compounds, $\{[\text{Co}(\text{PPDA})(\text{H}_2\text{O})_2]\}_n$ (**1**), $\{[\text{Ni}(\text{HPPDA})_2]\}_n$ (**2**), $\{[\text{Cd}(\text{PPDA})(\text{H}_2\text{O})]\cdot\text{H}_2\text{O}\}_n$ (**3**), and $\{\text{Zn}(\text{HPPDA})_2(\text{H}_2\text{O})_4\}_n$ (**4**), were synthesized by assembling transition metal salts with a semirigid ligand 4-(pyridin-3-yloxy)-phthalic acid (H_2PPDA) under hydrothermal conditions. The compounds have been characterized by elemental analyses, IR spectra, TGA, powder X-ray diffraction, and single-crystal X-ray crystallography. Compound **1** exhibits a three-connected 2-D layered structure, **2** shows a (3,6)-connected 2-D layered structure, **3** displays a (3,6)-connected 2-D layered framework based on binuclear units, and **4** is a mononuclear structure, connected to generate a 3-D supramolecular architecture by hydrogen bonds. Compound **2** is thermally stable up to 300 °C. The magnetic properties of **1** and photoluminescent properties of **3** and **4** have been explored.

Keywords: Coordination compounds; Semirigid ligand; Crystal structure; Luminescence; Magnetic property

1. Introduction

Design and construction of metal–organic frameworks (MOFs) are important in coordination chemistry, owing to their intriguing architectures and promising applications as functional materials in many fields, including catalysis, magnetism, gas adsorption, and

*Corresponding author. Email: hm988@126.com

luminescence [1–6]. However, the synthesis of MOFs with desirable structures and properties is still a challenging task for chemists. In the process of self-assembling, many factors, such as pH, solvent, temperature, reagent concentration, and the ratios between metal salts and ligands, have an unpredictable impact on the crystallization of coordination polymers [7]. Semirigid ligands have been extensively used for synthesis of coordination polymers because their restricted conformational variations facilitate the construction of high-dimensional coordination polymers [8, 9]. Ligands simultaneously containing pyridyl N and carboxylate donors are often selected as the organic linkers for their abundant coordination modes with metal centers to fabricate various topologies; 4,4'-bipyridine-2,2',6,6'-tetracarboxylic acid and analogs are frequently employed for the synthesis of coordination polymers [10–13].

We chose 4-(pyridin-3-yloxy)-phthalic acid (H_2PPDA) as ligand for the preparation of coordination polymers. The H_2PPDA possesses a pyridyl nitrogen and two carboxylic groups, which may give a variety of coordination modes with metal ions. H_2PPDA is considered as a semirigid ligand with restricted twisting along the C–O–C bond to allow formation of different structures constructed from pyridyl nitrogen and carboxylate. Crystal structures of coordination compounds based on H_2PPDA ligand are first reported here.

Four new coordination compounds have been synthesized under hydrothermal conditions, $\{[Co(PPDA)(H_2O)_2]\}_n$ (**1**), $\{[Ni(HPPDA)_2]\}_n$ (**2**), $\{[Cd(PPDA)(H_2O)] \cdot H_2O\}_n$ (**3**), AND $\{Zn(HPPDA)_2(H_2O)_4\}_n$ (**4**). The crystal structures, topological analyses, and thermal properties of **1–4** are studied and magnetic properties of **1** and the luminescence of **3** and **4** have also been explored.

2. Experimental

2.1. Materials and physical measurements

The chemical reagents and metal salts were commercially available and used without purification. Infrared spectra within the frequency range $4000\text{--}400\text{ cm}^{-1}$ were recorded on a Nicolet Avatar-360 spectrometer. Elemental analyses (C, H, and N) were performed on a Perkin-Elmer 2400 analyzer. Thermogravimetric analysis (TGA) was measured on a Perkin-Elmer TG-7 analyzer from 25 to $900\text{ }^\circ\text{C}$ under air. The fluorescence spectra were measured on a FLS920 fluorescence spectrophotometer.

Single-crystal X-ray diffraction data for **1–4** were collected on a Bruker Smart 1000 diffractometer using graphite-monochromatic Mo $K\alpha$ radiation ($\lambda = 0.71073\text{ \AA}$) at room temperature. Semiempirical absorption corrections were applied using SADABS. All of the structures were resolved by direct methods using SHELXS-97 and refined by full-matrix least squares fitting on $|F|^2$ by SHELXTL-97 [14]. All non-hydrogen atoms were refined anisotropically. The organic hydrogens were geometrically generated and hydrogens of water were located from difference Fourier maps and refined with the common isotropic thermal parameter. The crystal parameters, data collection, and refinement for **1–4** are summarized in table 1. Selected bond lengths and angles of **1–4** are listed in table S1. The data of hydrogen bonds in crystal packing for **4** are listed in table S2.

Table 1. Crystal data and structure refinement for **1–4**.

Compound	1	2	3	4
Empirical formula	C ₁₃ H ₁₁ NO ₇ Co	C ₂₆ H ₁₆ N ₂ O ₁₀ Ni	C ₁₃ H ₉ NO ₆ Cd	C ₂₆ H ₂₄ N ₂ O ₁₄ Zn
Formula weight	352.16	575.10	405.64	653.86
Temperature (K)	293	293	296	293
Crystal system	Monoclinic	Monoclinic	Monoclinic	Triclinic
Space group	<i>P</i> 2 ₁ / <i>c</i>	<i>C</i> 2	<i>P</i> 2 ₁ / <i>c</i>	<i>P</i> -1
Unit-cell dimensions (Å, °)	<i>a</i> = 13.2272(7) <i>b</i> = 8.9240(5) <i>c</i> = 11.3571(7) <i>α</i> = 90 <i>β</i> = 93.215(6) <i>γ</i> = 90	<i>a</i> = 18.168(2) <i>b</i> = 8.4404(10) <i>c</i> = 7.5365(6) <i>α</i> = 90 <i>β</i> = 102.297(14) <i>γ</i> = 90	<i>a</i> = 8.9571(15) <i>b</i> = 20.340(3) <i>c</i> = 7.9173(13) <i>α</i> = 90 <i>β</i> = 102.925(3) <i>γ</i> = 90	<i>a</i> = 8.333(3) <i>b</i> = 9.327(4) <i>c</i> = 10.088(4) <i>α</i> = 77.045(6) <i>β</i> = 72.955(6) <i>γ</i> = 64.316(6)
Volume (Å ³)	1338.48(13)	1129.2(2)	1405.9(4)	671.2(5)
<i>Z</i>	4	2	4	1
Density (calculated) (g cm ⁻³)	1.748	1.692	1.916	1.622
Absorption coefficient (mm ⁻¹)	1.319	0.929	1.589	0.994
<i>F</i> (0 0 0)	716	588	800	338
<i>θ</i> range for data collection	2.75–24.99	2.67–25.00	2.00–28.32	2.13–28.43
Reflections collected/unique	4829/2355	3654/1903	10,104/3488	9310/3333
Data/restraints/parameters	2355/0/201	1903/483/181	3488/0/203	3333/1/199
Goodness-of-fit on <i>F</i> ²	1.075	1.119	1.184	1.031
Final <i>R</i> indices [<i>I</i> > 2σ(<i>I</i>)]	<i>R</i> 1 = 0.0453 <i>wR</i> 2 = 0.0908	<i>R</i> 1 = 0.0486 <i>wR</i> 2 = 0.1183	<i>R</i> 1 = 0.0225 <i>wR</i> 2 = 0.0514	<i>R</i> 1 = 0.0392 <i>wR</i> 2 = 0.0913
<i>R</i> indices (all data)	<i>R</i> 1 = 0.0679 <i>wR</i> 2 = 0.1060	<i>R</i> 1 = 0.0583 <i>wR</i> 2 = 0.1294	<i>R</i> 1 = 0.0234 <i>wR</i> 2 = 0.0517	<i>R</i> 1 = 0.0524 <i>wR</i> 2 = 0.0959

2.2. Synthesis of $\{[Co(PPDA)(H_2O)_2]\}_n$ (**1**)

A mixture of Co(CH₃COO)₂·4H₂O (0.20 mmol, 49.8 mg), H₂PPDA (0.20 mmol, 51.8 mg), and 5.0 mL of H₂O was sealed in a 23-mL Teflon-lined stainless steel container stirred for 30 min in air, heated at 140 °C for 72 h, and then cooled to 30 °C at a rate of 2 °C h⁻¹. After filtration, the product was washed with distilled water and then air dried; red block crystals of **1** were obtained suitable for single-crystal X-ray diffraction analysis, 46 mg for yield of 66%. Elemental analysis (%): Calcd for C₁₃H₁₁NO₇Co: C, 44.38; H, 3.22; N, 3.84. Found: C, 44.29; H, 3.12; N, 3.98. IR (KBr, cm⁻¹): 3446(s), 1669(m), 1612(s), 1548(s), 1491(m), 1476(m), 1423(s), 1398(s), 1269(m), 1248(m), 890(m), 704(m), 609(m).

2.3. Synthesis of $\{[Ni(HPPDA)_2]\}_n$ (**2**)

A mixture of Ni(ClO₄)₂·6H₂O (0.30 mmol, 71.3 mg), H₂PPDA (0.30 mmol, 77.7 mg), and 5.0 mL of H₂O was sealed in a 23-mL Teflon-lined stainless steel container stirred for 30 min in air, heated at 140 °C for 72 h, and then cooled to 30 °C at a rate of 2 °C h⁻¹. Bright green diamond-shaped single crystals of **2** suitable for single-crystal X-ray diffraction were isolated by filtration, washed with distilled water several times, and then air dried, 103 mg for yield of 60%. Elemental analysis (%): Calcd for C₂₆H₁₆N₂O₁₀Ni: C, 54.25; H, 2.78; N, 4.87. Found: C, 54.55; H, 2.65; N, 4.98. IR (KBr, cm⁻¹): 3440(s), 1710(m), 1598(s), 1557(s), 1447(s), 1434(s), 1385(s), 1262(s), 1263(m), 1208(m), 899(m), 766(m), 727(m), 699(s).

2.4. Synthesis of $\{[Cd(PPDA)(H_2O)]\cdot H_2O\}_n$ (**3**)

A mixture of Cd(NO₃)₂·4H₂O (0.05 mmol, 15.4 mg), H₂PPDA (0.05 mmol, 12.9 mg), and 4.0 mL of H₂O/CH₃CN (1 : 1, v:v) was sealed in a 23-mL Teflon-lined stainless steel

container stirred for 30 min in air, heated at 165 °C for 100 h, and cooled to 30 °C at a rate of 2 °C h⁻¹. After filtration, the product was washed with distilled water and then air dried; bright yellow block crystals of **3** were obtained suitable for single-crystal X-ray diffraction analysis, 14 mg for yield of 70%. Elemental analysis (%): Calcd for C₁₃H₉NO₆Cd: C, 38.46; H, 2.22; N, 3.45. Found: C, 38.55; H, 2.13; N, 3.56. IR (KBr, cm⁻¹): 3443(m), 1548(s), 1483(w), 1413(s), 1250(s), 1196(m), 949(m), 854(m), 791(m), 686(m), 538(m).

2.5. Synthesis of $\{[Zn(HPPDA)_2(H_2O)_4]\}_n$ (**4**)

A mixture of ZnSO₄·7H₂O (0.20 mmol, 57.6 mg), H₂PPDA (0.20 mmol, 51.8 mg), and 5.0 mL of H₂O was sealed in a 23-mL Teflon-lined stainless steel container stirred for 30 min in air, heated at 120 °C for 72 h, kept 24 h at 80 °C, and then slowly cooled to room temperature at a rate of 5 °C h⁻¹. After filtration, the product was washed with distilled water and air dried; yellow block crystals of **4** were obtained suitable for single-crystal X-ray diffraction analysis, 65 mg for yield of 50%. Elemental analysis (%): Calcd for C₂₆H₂₄N₂O₁₄Zn: C, 47.72; H, 3.67; N, 4.28. Found: C, 47.65; H, 3.66; N, 4.14. IR (KBr, cm⁻¹): 3381(m), 1705(m), 1676(m), 1585(s), 1557(s), 1488(s), 1438(s), 1365(s), 1269(s), 1234(m), 1024(w), 1057(w), 954(m), 776(m), 683(m).

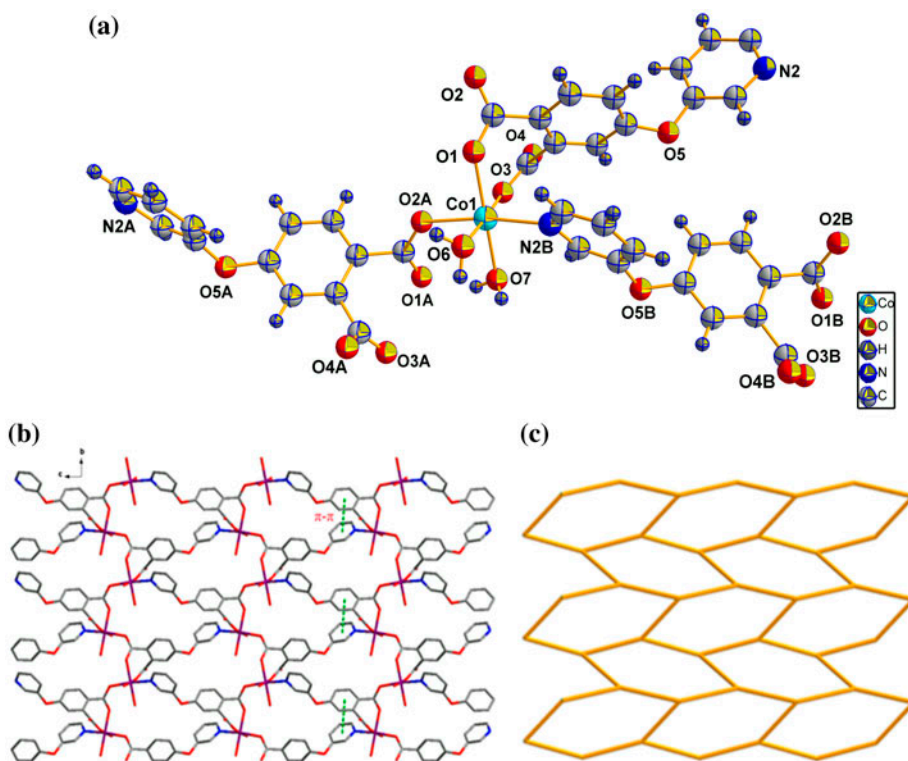


Figure 1. (a) Coordination environment of Co(II) with 50% probability ellipsoids; (b) 2-D layer structure in **1** along the *a*-axis; and (c) Schematic representation of the 3-connected network.

3. Results and discussion

3.1. Crystal structure of **1**

Single-crystal X-ray diffraction analysis reveals that **1** is in the monoclinic system with space group $P2_1/c$. The asymmetric unit contains an independent Co(II), a PPDA²⁻, and two coordinated waters. The coordination environment of Co(II), shown in figure 1(a), is six coordinate with three carboxylate oxygens (O1, O2A, and O3) belonging to the PPDA²⁻ ligands in which O1 and O3 are from one PPDA²⁻ and O2A from another PPDA²⁻, a nitrogen (N2B) from PPDA²⁻, and O6 and O7 from coordinated water, in a slightly distorted octahedral geometry. The Co–O (water) bond length is 2.102 Å, Co–O (bridging carboxylate) bond lengths are 2.087 and 2.162 Å, Co–O (monodentate) bond length is 2.056 Å, and Co–N distance is 2.174(4) Å, which are well matched to those observed in similar complexes [15]. The C–O–C angle between the pyridyl ring and aromatic ring is 118.72°. The two carboxylate groups are distorted with the linking aromatic ring, and the dihedral angles between carboxylate groups and aromatic rings are 63.75° and 56.77°, respectively. The completely deprotonated carboxylate groups of PPDA²⁻ adopt monodentate and bridging bidentate modes [scheme 1(a)]. Co(II) ions are connected through carboxylate oxygens (O1, O2A) to lead to 1-D chains; adjacent 1-D chains are further linked by carboxylate oxygen (O3) and nitrogen of the pyridyl ring to generate a 2-D layer viewed along the *a*-axis [figure 1(b)]. There are π - π interactions between pyridyl rings and aromatic rings, the distance between centroids is 3.8076 Å [16]. Moreover, the neighboring 2-D layers are further connected through hydrogen bonds between coordinated water molecules and carboxylate oxygen atoms to generate a 3-D network. From the topological point of view, each Co(II) is ligated by three ligands, which can be considered as a three-connected node; each PPDA²⁻ connects with three Co centers and thus can be defined as a three-connected node. According to this simplification, the whole framework of **1** can be described as a network with a Schläfli symbol of $\{6^3\}$, as illustrated in figure 1(c).

3.2. Crystal structure of **2**

Polymer **2** crystallizes in the monoclinic system and space group $C2$. H₂PPDA ligands are deprotonated to HPPDA⁻. The asymmetric unit of **2** contains an independent Ni(II) and HPPDA⁻ ligands. Ni(II) is six coordinate with four oxygens (O1, O1A, O4B, O4C) of four ligands and two N (N1D, N1E) from two different ligands [figure 2(a)]. The carboxylate groups of HPPDA⁻ are monodentate [scheme 1(b)] to bridge Ni(II) centers to form a 1-D chain. Nitrogens and carboxylate groups of HPPDA⁻ connect the neighboring 1-D chains to generate a 2-D layer, as shown in figure 2(b). The Ni–O bond distances are 2.069(5) and 2.080(5) Å and the Ni–N bond length is 2.090(4) Å, consistent with reported complexes [17]. Adjacent Ni \cdots Ni distances are 8.44 and 11.31 Å, respectively. The C–O–C angle between pyridyl ring and aromatic ring is 119.49°. Every carboxylate group is distorted with the linking aromatic ring, and the dihedral angles between the carboxylate groups and aromatic rings are 16.09 and 17.53°, respectively. Considering Ni(II) ions and HPPDA⁻ ligands as three- and six-connecting nodes, the structure of **2** can be simplified as a binodal topological net with a Schläfli symbol of $\{4^3\}_2\{4^66^68^3\}$, as shown in figure 2(c). The framework of **2** possesses the common topological binodal *kgd* net.

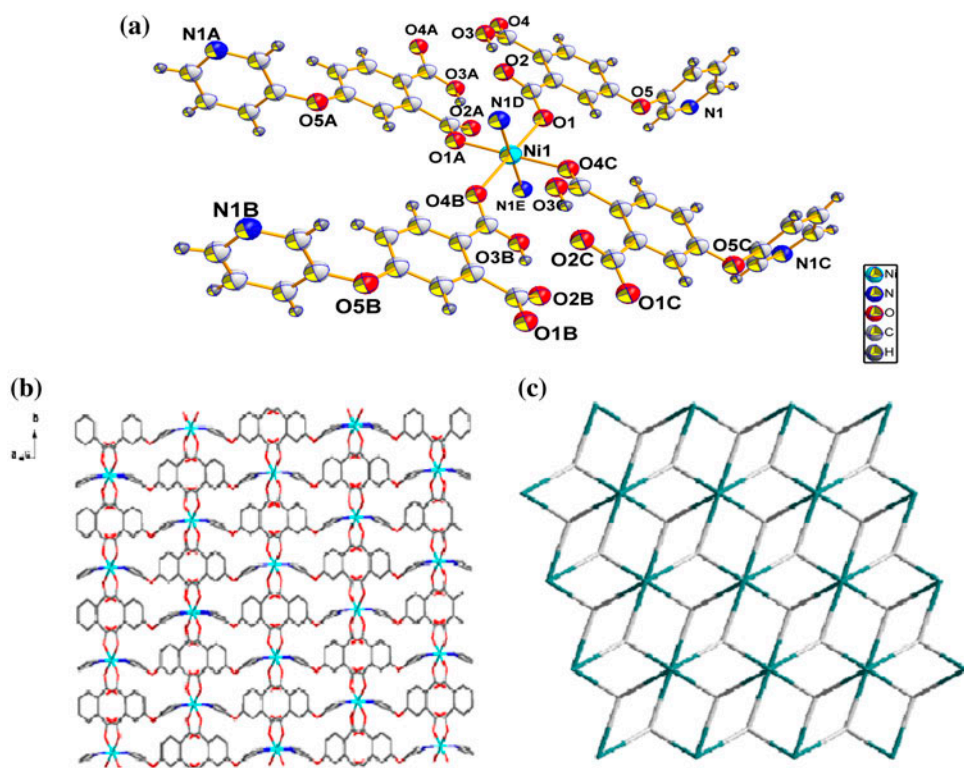


Figure 2. (a) Coordination environment of Ni(II) in **2** with 50% probability ellipsoids; (b) 2-D layer structure in **2** viewed in the *ab*-plane; and (c) Simplified (3,6)-coordinated single net.

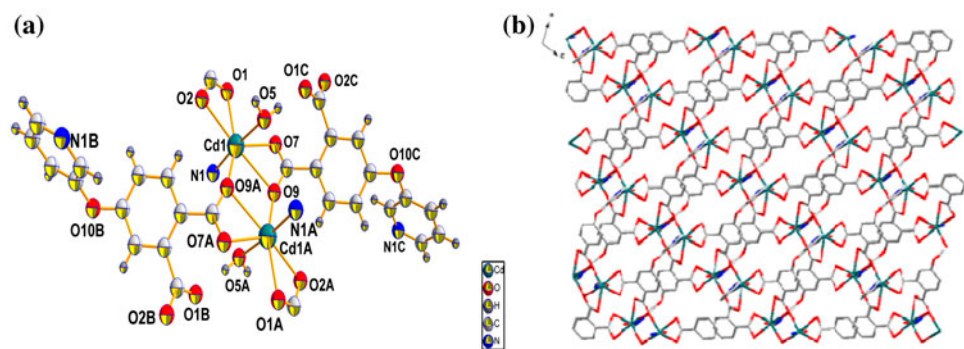


Figure 3. (a) Coordination environment of Cd(II) in **3** with 50% probability ellipsoids and (b) 2-D layer structure in **3** viewed in the *b*-direction.

3.3. Crystal structure of **3**

Single-crystal X-ray diffraction analysis demonstrates that **3** crystallizes in monoclinic $P2_1/c$ space group. The asymmetric unit contains a Cd(II), three PPDA²⁻ ligands, a

coordinated water, and a free water. As illustrated in figure 3(a), Cd(II) is seven coordinate by five carboxylate oxygens (O1, O2, O7, O9, O9A) from three PPDA²⁻ ligands, O5 from coordinated water, and N1 from PPDA²⁻ in a pentagonal bipyramid. The Cd–O (chelating/bridging tridentate) distances are 2.2710(15), 2.4194(15), and 2.6042(16) Å, Cd–O (chelating bidentate) bond lengths are 2.3731(15) and 2.4679(16) Å, Cd–O(water) length is 2.2801(15) Å, and Cd–N distance is 2.2809(18) Å, all in the normal reported ranges [18]. The C–O–C angle between pyridyl ring and aromatic ring is 116.83°. Every carboxylate group is distorted with the linked aromatic ring, the dihedral angles between carboxylate groups and aromatic rings are 27.06° and 53.39°, respectively. The two carboxylate groups of PPDA²⁻ show two coordination modes to link the binuclear Cd(II) units; one is a chelating bidentate mode and the other is a chelating/bridging tridentate mode, where O9 is μ_2 -O [scheme 1(c)], forming a binuclear Cd₂O₂ moiety; the Cd(II) ions in Cd₂O₂ moiety are 3.9298(5) Å apart. Each binuclear Cd₂O₂ moiety is further linked through six PPDA²⁻ ligands to generate a 2-D layered structure [figure 3(b)]. From the topological point of view, each binuclear Cd unit is ligated by six PPDA²⁻ ligands, which can be considered as 6-connected nodes; each PPDA²⁻ anion connects to three binuclear Cd(II) units, the PPDA²⁻ ligand can be defined as a three-connected node. Therefore, the structure of **3** can be simplified as a binodal topological network. Compound **3** displays similar topological structure to **2**.

3.4. Crystal structure of **4**

Complex **4** crystallizes in triclinic symmetry with space group *P*-1. The asymmetric unit contains an independent Zn(II), a HPPDA⁻, and coordinated water, as shown in figure 4(a). Zn(II) is six coordinate with two nitrogens (N1 and N1A) belonging to HPPDA⁻ ligands and four water molecules in a slightly distorted octahedron. Two nitrogens from HPPDA⁻ ligands occupy the axial positions of octahedral geometry. The horizontal plane of the octahedron has water molecules. The Zn–O bond lengths are in the range of 2.1037(16)–2.1086(16) Å and the Zn–N distance is 2.1506(18) Å. Both Zn–O and Zn–N bond lengths are well matched to those observed in similar complexes [19]. The C–O–C angles between the pyridyl ring and aromatic ring is 118.94°. Every carboxylate is distorted with the linking aromatic ring, and the dihedral angles between the carboxylate groups and aromatic rings

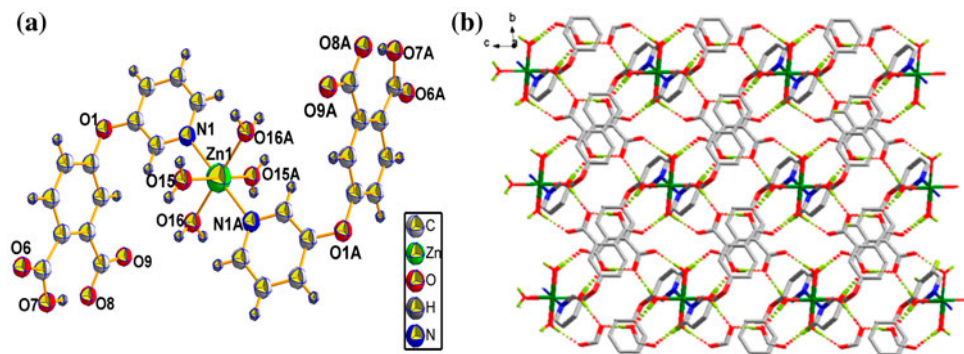


Figure 4. (a) Coordination environment of Zn(II) in **4** with 50% probability ellipsoids and (b) 3-D supramolecular structure of **4** connected by hydrogen bonds along the *a*-axis.

are 8.87° and 9.05°. Only the nitrogen of pyridyl ring coordinates with Zn(II) center [scheme 1(d)]. The 3-D supramolecular structure is formed by hydrogen bonds between HPPDA⁻ ligands and coordinated water, connecting Zn(HPPDA)₂(H₂O)₄ to form a 3-D supramolecular structure, as shown in figure 4(b). Hydrogen bonds are with the carboxylate O7 and O8; coordinated water O15, O16, and carboxylate O6, O7, O8, O9. (O7...O8, 2.386 Å; O15...O7, 2.731 Å; O15...O8, 2.776 Å; O16...O6, 2.740 Å; O16...O9, 2.720 Å).

Complexes 1–4 display a mononuclear and three 2-D layers. The variations originate from the distinct coordination environments of metal centers and deprotonation of H₂PPDA; the results demonstrate that HPPDA⁻ and HPPDA²⁻ adopt the diverse coordination modes to bind the metal centers in 1–4. The semirigidity of ligand also contributes to the dissimilar structures of 1–4.

3.5. Thermogravimetric analysis

To examine the thermal stabilities of 1–4, TGA were carried out from ambient temperature to 900 °C at 5 °C per minute in air (figure 5). The TGA of 1 shows that two coordinated waters are lost at 130 °C (obsd. 10.3%, Calcd 10.2%). The further exothermal process begins at 260 °C, attributed to decomposition of the ligand (obsd. 69.2%, Calcd 68.5%). With increasing temperature, the framework is totally decomposed and the final product of 1 is CoO (obsd. 20.5%, Calcd 21.3%). For 2, the framework of complex is stable at 300 °C because there are no solvent molecules or coordination water molecules. With rising temperature, the ligand is broken completely down (obsd. 85.4%, Calcd 87.1%) and the product is NiO (obsd. 14.6%, Calcd 12.9%). Compound 2 shows extraordinary thermal stability. For 3, the first step before 100 °C is assigned to the loss of one lattice water and one coordinated water (obsd. 9.9%, Calcd 8.9%), the second step starts at 280 °C, corresponding to the decomposition of ligand and the final residue is CdO (obsd. 30.4%, Calcd

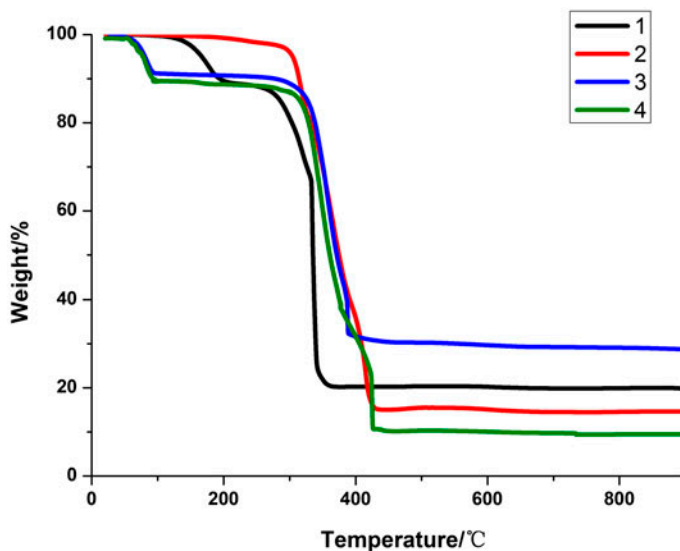


Figure 5. The TGA curves of 1–4.

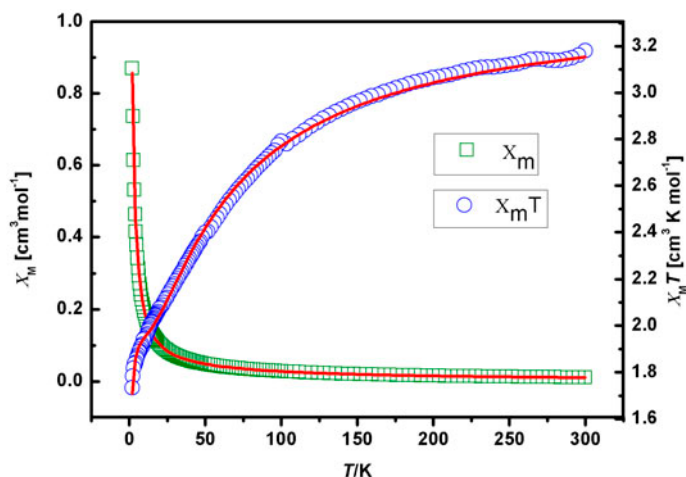


Figure 6. Temperature dependence of $\chi_m T$ and χ_m for **1**. Open points are the experimental data.

31.6%). For **4**, the weight loss before 100 °C is attributed to the loss of four coordinated waters (obsd. 10.7%, Calcd 11.0%). Then, collapse of the network of **4** is at 300 °C and the product is ZnO (obsd. 10.5%, Calcd 12.4%). In order to check the phase purity of **1–4**, the powder X-ray diffraction patterns were checked at room temperature, as shown in figures S1–S4.

3.6. Magnetism

The magnetic properties of **1** were investigated from 2.0 to 300.0 K under 1000 Oe. As shown in figure 6, the $\chi_m T$ value of **1** at 300 K is 3.18 cm³ K mol⁻¹, larger than the

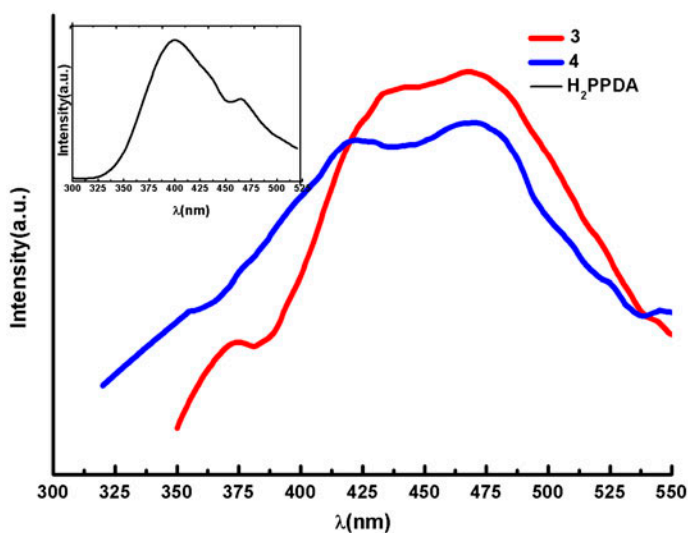
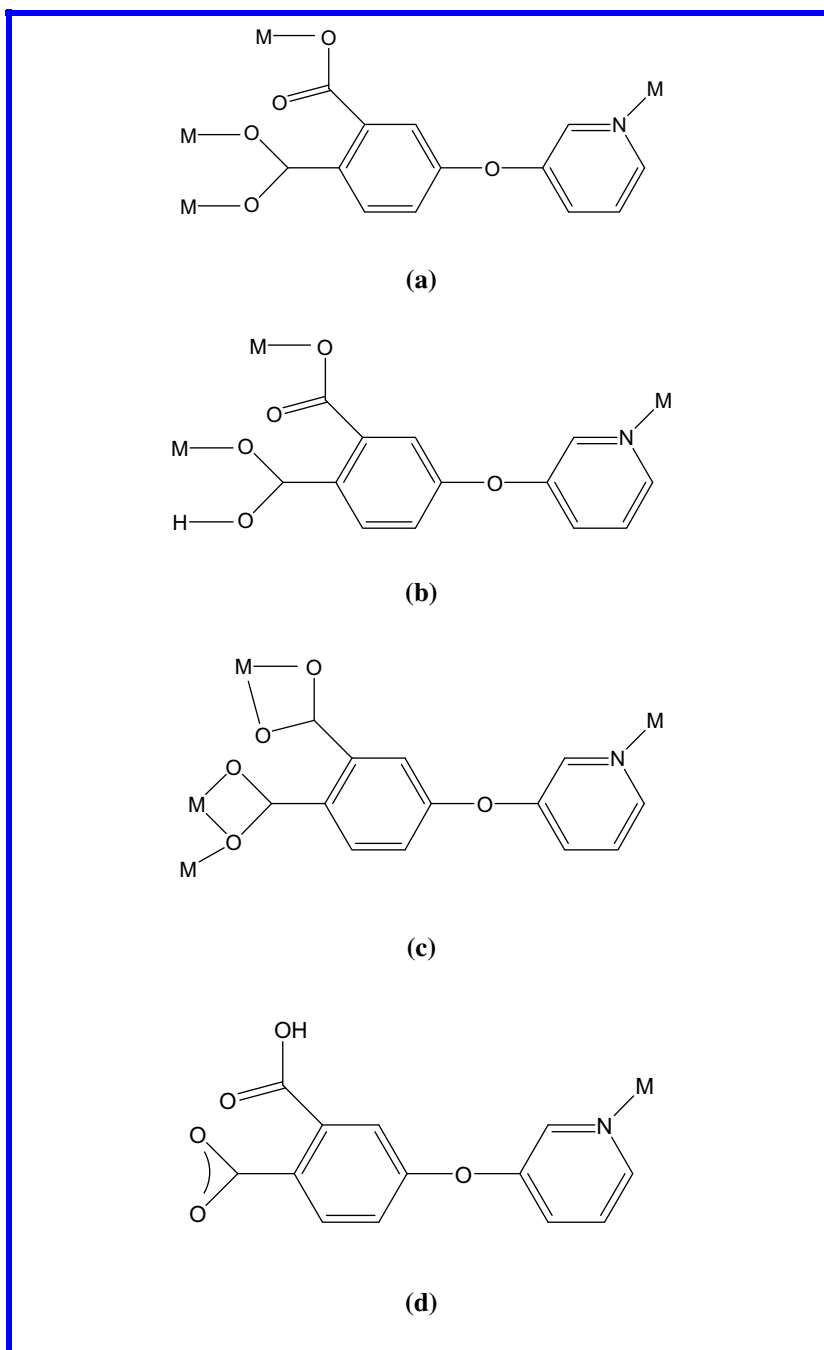


Figure 7. Photoluminescence spectra of **3**, **4**, and H₂PPDA in the solid state.

Scheme 1. Coordination modes of HPPDA⁻ and PPDA²⁻ in 1–4.

expected value of $1.88 \text{ cm}^3 \text{ K mol}^{-1}$ with $g = 2.00$. The larger experimental value of **1** than corresponding spin only value can be attributed to the unquenched orbital moment, as a result of spin-orbit coupling in the distorted octahedral Co(II) ions [20]. Upon decreasing the temperature, the $\chi_m T$ value of **1** continuously decreases and reaches a minimum of $1.7 \text{ cm}^3 \text{ K mol}^{-1}$ at 2.0 K. Between 25 and 300 K, the χ_m^{-1} versus T data can be fitted by the Curie-Weiss law with $C = 3.41 \text{ cm}^3 \text{ K mol}^{-1}$ and $\theta = -22.81 \text{ K}$. The negative Weiss constant is the evidence of antiferromagnetic interactions between Co(II) ions. From 2.0 to 300 K, the temperature dependence of the $\chi_m T$ value was roughly fitted to the simple equation [21]:

$$\chi_m T = A e^{-E_1/KT} + B e^{-E_2/KT}$$

Here, $A + B$ is the Curie constant, and E_1 and E_2 represent the activation energies corresponding to the spin-orbit coupling and the magnetic exchange interaction, respectively [22]. This equation adequately describes the spin-orbit coupling, which results in a splitting between discrete levels. Moreover, it is in excellent agreement with the experimental data obtained in the present work (figure 6). The obtained values are $A = 1.40 \text{ cm}^3 \text{ K mol}^{-1}$, $B = 2.01 \text{ cm}^3 \text{ K mol}^{-1}$, $E_1 = 41.83 \text{ cm}^{-1}$, $E_2 = 0.22 \text{ cm}^{-1}$, and Curie constant $C = 3.41 \text{ cm}^3 \text{ K mol}^{-1}$. The values found for $C = A + B$ agree with those obtained from the Curie-Weiss law and the values for E_1/k ($E_1/k = 60.18 \text{ K}$, using a least-squares fitting method) are consistent with those given in the literature for both the effects of spin-orbit coupling and site distortion (E_1/k of the order of 100 K). The small E_2 value indicates the presence of weak antiferromagnetic interaction [23, 24].

3.7. Luminescent properties

As shown in figure 7, the solid-state luminescence spectra of **3**, **4**, and H₂PPDA have been determined at room temperature. H₂PPDA displays very weak photoluminescence with emission maximal peak at 400 nm and a shoulder at 464 nm ($\lambda_{\text{ex}} = 270 \text{ nm}$), which could be attributed to intraligand $\pi^*-\pi$ and π^*-n transitions. Compound **3** exhibits emission bands at 435 and 468 nm ($\lambda_{\text{ex}} = 328 \text{ nm}$). The obvious red shifted emission at 435 nm compared with the emission band of H₂PPDA ligand at 400 nm could be assigned to the ligand-to-metal charge transfer (LMCT); furthermore, the emission peak of 468 nm can be attributed to the intraligand fluorescent emission [25, 26]. Compound **4** shows dual emission bands, one centered at 419 nm, which is red shifted at 19 nm comparing with that of H₂PPDA ligand and is caused by LMCT; another is at 471 nm, which is assigned to the intraligand transitions ($\lambda_{\text{ex}} = 300 \text{ nm}$). The strong luminescence of **3** and **4** makes them candidates for potential functional materials.

4. Conclusion

Four new coordination compounds generated from a semirigid ligand with different transition metal salts under hydrothermal conditions display diverse structures. Polymers **1** and **2** show 2-D layered structure, **3** is a binuclear 2-D layered architecture and **4** displays a mononuclear structure. Magnetic properties of **1** reveal antiferromagnetic interactions between Co(II) ions. The photoluminescent properties of **3** and **4** could be assigned to LMCT and intraligand charge transitions.

Supplementary material

CCDC 958937-958940 for 1–4 contain the supplementary crystallographic data. These data can be obtained free of charge via <http://www.ccdc.cam.ac.uk/conts/retrieving.html>, or from the CCDC, 12 Union Road, Cambridge CB21EZ, UK; Fax: +441223-336-033; or E-mail: deposit@ccdc.cam.ac.uk.

Disclosure statement

No potential conflict of interest was reported by the authors.

Funding

This work was financially supported by the National Natural Science Foundation of China [grant number 21361017]; Inner Mongolia Natural Science Foundation of China [grant number 2014BS0206]; Scientific and Technological Key Research Project of Inner Mongolia Colleges & Universities [grant number NJZZ12012].

Supplemental data

Supplemental data for this article can be accessed at <http://dx.doi.org/10.1080/00958972.2015.1081183>.

References

- [1] (a) M. O'Keefe, O.M. Yaghi. *Chem. Rev.*, **112**, 675 (2012); (b) K.H. Wang, E.J. Gao. *J. Coord. Chem.*, **67**, 563 (2014); (c) D. Zhao, D.J. Timmons, D. Yuan, H.C. Zhou. *Acc. Chem. Res.*, **44**, 123 (2011); (d) B. Wang, Y.B. Xie, H. Yang. *J. Coord. Chem.*, **67**, 3484 (2014).
- [2] (a) J.J. Perry IV, J.A. Perman, M.J. Zaworotko. *Chem. Soc. Rev.*, **38**, 1400 (2009); (b) P.F. Yao, C.J. Ye, F.P. Huang. *J. Coord. Chem.*, **66**, 1591 (2014); (c) X.Z. Yan, D.H. Xu, J.Z. Chen, M.M. Zhang, B.J. Hu, Y.H. Yu, F.H. Huang. *Polym. Chem.*, **4**, 3312 (2013); (d) S.M. Keltie, P.A. Gale, M.E. Light. *J. Coord. Chem.*, **66**, 3058 (2014).
- [3] (a) M.D. Allendorf, C.A. Bauer, R.K. Bhakta, R.J.T. Houk. *Chem. Soc. Rev.*, **38**, 1330 (2009); (b) J.H. Zhou, Y. Wang, S.N. Wang. *J. Coord. Chem.*, **66**, 737 (2014); (c) X.Z. Yan, D.H. Xu, X.D. Chi, J.Z. Chen, S.Y. Dong, X. Ding, Y.H. Yu, F.H. Huang. *Adv. Mater.*, **24**, 362 (2012); (d) Y.H. Yu, B. Wen, H.Z. Zhang. *J. Coord. Chem.*, **67**, 588 (2014).
- [4] (a) H.Y. Liu, Z.J. Zhang, W. Shi, B. Zhao, P. Cheng, D.Z. Liao, S.P. Yan. *Dalton Trans.*, **23**, 4416 (2009); (b) A. Morsali, M.Y. Masoomi. *Coord. Chem. Rev.*, **253**, 1882 (2009); (c) J.F. Eubank, H. Mouttaki, A.J. Cairns, Y. Belmabkhout, L. Wojtas, R. Luebke, M. Alkordi, M. Eddaoudi. *J. Am. Chem. Soc.*, **133**, 14204 (2011); (d) M.Y. Masoomi, K.C. Stylianou, A. Morsali, P. Retailleau, D. Maspoch. *Cryst. Growth Des.*, **14**, 2092 (2014).
- [5] (a) M.H. Zeng, Z. Yin, Y.X. Tan. *J. Am. Chem. Soc.*, **136**, 4680 (2014); (b) Y.Q. Mu, B.F. Zhu, D.S. Li, D. Guo, J. Zhao, L.F. Ma. *Inorg. Chem. Commun.*, **33**, 86 (2013); (c) F. Sun, Z. Yin, Q.Q. Wang. *Angew. Chem. Int. Ed.*, **52**, 4538 (2013); (d) M.Y. Masoomi, A. Morsali, P.C. Junk. *RSC Adv.*, **4**, 47894 (2014).
- [6] (a) A. Kajbafvala, H. Ghorbani, A. Paravar, J.P. Samberg, E. Kajbafvala, S.K. Sadrnezhaad. *Superlattices Microstruct.*, **51**, 512 (2012); (b) X.Z. Yan, F. Wang, B. Zheng, F.H. Huang. *Chem. Soc. Rev.*, **41**, 6042 (2012); (c) Z. Yin, Q.X. Wang, M.H. Zeng. *J. Am. Chem. Soc.*, **134**, 4857 (2012); (d) N. Stock, S. Biswas. *Chem. Rev.*, **112**, 933 (2012); (e) M.Y. Masoomi, A. Morsali. *Coord. Chem. Rev.*, **256**, 2921 (2012).
- [7] (a) Z.L. Fang, J.G. He, Q.S. Zhang, Q.K. Zhang, X.Y. Wu, R.M. Yu, C.Z. Lu. *Inorg. Chem.*, **50**, 11403 (2011); (b) P.X. Yin, J. Zhang, Y.Y. Qin, J.K. Cheng, Z.J. Li, Y.G. Yao. *CrystEngComm*, **13**, 3536 (2011); (c) S.L. Li, K. Tan, Y.Q. Lan, J.S. Qin, M.N. Li, D.Y. Du, H.Y. Zang, Z.M. Su. *Cryst. Growth Des.*, **10**, 1699 (2010).
- [8] (a) Q.X. Yang, X.Q. Chen, Z.J. Chen, Y. Hao, Y.Z. Li, Q.Y. Lu, H.G. Zheng. *Chem. Commun.*, **48**, 10016 (2012); (b) X. Feng, X.L. Ling, B. Liu, Z.Q. Shi, J.J. Shang, L.Y. Wang. *Inorg. Chem. Commun.*, **20**, 1 (2012).
- [9] (a) Z.J. Lin, L.W. Han, D.S. Wu, Y.B. Huang, R. Cao. *Cryst. Growth Des.*, **13**, 255 (2013); (b) L.L. Wen, Z.D. Lu, J.G. Lin, Z.F. Tian, H.Z. Zhu, Q.J. Meng. *Cryst. Growth Des.*, **7**, 93 (2007).

- [10] (a) C. Yang, F.P. Huang, H.Y. Li. *J. Coord. Chem.*, **66**, 3939 (2014); (b) Z. Zhao, X. He, Y.M. Zhao, M. Shao, S.R. Zhu. *Dalton Trans.*, **15**, 2802 (2009); (c) B. Zhao, H.L. Gao, X.Y. Chen, P. Cheng, W. Shi, D.Z. Liao, S.P. Yan, Z.H. Jiang. *Chem. Eur. J.*, **12**, 149 (2006).
- [11] (a) B.M. Ji, D.S. Deng, X. He, B. Liu, S.B. Miao, N. Ma, W.Z. Wang, L.G. Ji, P. Liu, X.F. Li. *Inorg. Chem.*, **51**, 2170 (2012); (b) H.W. Kuai, X.Y. Xu, X.C. Cheng. *J. Coord. Chem.*, **66**, 4304 (2014).
- [12] (a) M. Chen, Z.S. Bai, Q. Liu, T. Okamura, Y. Lu, W.Y. Sun. *CrystEngComm*, **14**, 8642 (2012); (b) X.Y. Lu, J.W. Ye, L.M. Zhao. *J. Coord. Chem.*, **67**, 1133 (2014).
- [13] (a) Y. Cui, Y. Yue, G. Qian, B. Chen. *Chem. Rev.*, **112**, 1126 (2012); (b) C. Butler, S. Goetz, C.M. Fitchett, P.E. Kruger, T. Gunnlaugsson. *Inorg. Chem.*, **50**, 2723 (2011).
- [14] G.M. Sheldrick. *SHELXS-97, Program for X-ray Crystal Structure Solution*, University of Göttingen, Germany (1997).
- [15] (a) X.H. Bu, M.L. Tong, Y.B. Xie, J.R. Li, H.C. Chang, S. Kitagawa, J. Ribas. *Inorg. Chem.*, **44**, 9837 (2005); (b) W.X. Chen, G.L. Zhuang, H.X. Zhao, L.S. Long, R.B. Huang, L.S. Zheng. *Dalton Trans.*, **40**, 10237 (2011).
- [16] J.H. Deng, D.C. Zhong, X.Z. Luo, H.J. Liu, T.B. Lu. *Cryst. Growth Des.*, **12**, 4861 (2012).
- [17] (a) J.S. Guo, G. Xu, G.C. Guo, J.S. Huang. *Cryst. Growth Des.*, **13**, 2642 (2013); (b) M. Chen, Z.S. Bai, Q. Liu, T. Okamura, Y. Lu, W.Y. Sun. *CrystEngComm*, **14**, 8642 (2012).
- [18] (a) L.N. Li, S.Y. Wang, T.L. Chen, Z.H. Sun, J.H. Luo, M.C. Hong. *Cryst. Growth Des.*, **12**, 4109 (2012); (b) J.J. Han, Y.F. Niu, J. Han, X.L. Zhao. *Polyhedron*, **55**, 249 (2013).
- [19] X.J. Hong, M.F. Wang, H.Y. Jia, W.X. Li, J. Li, Y.T. Liu, H.G. Jin, Y.P. Cai. *New J. Chem.*, **37**, 933 (2013).
- [20] (a) M. Kurmoo. *Chem. Soc. Rev.*, **38**, 1353 (2009); (b) Z. Chen, Y. Li, C. Jiang, F. Liang, Y. Song. *Dalton Trans.*, **27**, 5290 (2009); (c) H.L. Wang, D.P. Zhang, D.F. Sun, Y.T. Chen, L.F. Zhang, L.J. Tian, J.Z. Jiang, Z.H. Ni. *Cryst. Growth Des.*, **9**, 5273 (2009).
- [21] S.Q. Zang, L.H. Cao, R. Liang, H.W. Hou, T.C.W. Mak. *Cryst. Growth Des.*, **12**, 1830 (2012).
- [22] (a) J.M. Rueff, N. Masciocchi, P. Rabu, A. Sironi, A. Skoulios. *Eur. J. Inorg. Chem.*, **11**, 2843 (2001); (b) P. Rabu, J.M. Rueff, Z.L. Huang, S. Angelov, J. Souletie, M. Drillon. *Polyhedron*, **20**, 1677 (2001).
- [23] J.M. Rueff, N. Masciocchi, P. Rabu, A. Sironi, A. Skoulios. *Chem. Eur. J.*, **8**, 1813 (2002).
- [24] Q. Chen, J.B. Lin, W. Xue, M.H. Zeng, X.M. Chen. *Inorg. Chem.*, **50**, 2321 (2011).
- [25] G.B. Che, C.B. Liu, B. Liu, Q.W. Wang, Z.L. Xu. *CrystEngComm*, **10**, 184 (2008).
- [26] S.Y. Song, X.Z. Song, S.N. Zhao, C. Qin, S.Q. Su, M. Zhu, Z.M. Hao, H.J. Zhang. *Dalton Trans.*, **41**, 10412 (2012).